


RESEARCH ARTICLE

Auditory neuropathy in mice and humans with Friedreich ataxia

Gary Rance¹ , Peter Carew¹, Leon Winata², Phillip Sale², Martin Delatycki³ & David Sly^{2,4}¹Department of Audiology and Speech Pathology, The University of Melbourne, Melbourne, Victoria, Australia²Department of Otolaryngology, University of Melbourne, Melbourne, Victoria, Australia³Victorian Clinical Genetics Services, Bruce Lefroy Centre for Genetic Health Research, Murdoch Children's Research Institute, Melbourne, Victoria, Australia⁴Ear Science Institute Australia, Perth, Western Australia, Australia**Correspondence**

Gary Rance, Department of Audiology and Speech Pathology, The University of Melbourne, Melbourne, VIC, Australia.

Tel: +61 3 9035 5342;

Fax: +61 3 9347 9736;

E-mail: grance@unimelb.edu.au

Received: 18 January 2023; Revised: 20 February 2023; Accepted: 8 March 2023

Annals of Clinical and Translational Neurology 2023; 10(6): 953–963

doi: 10.1002/acn3.51777

ABSTRACT

Objective: Recent studies have found that human Friedreich ataxia patients have dysfunction of transmission in the auditory neural pathways. Here, we characterize hearing deficits in a mouse model of Friedreich ataxia and compare these to a clinical population. **Methods:** Sixteen mice with a C57BL/6 background were evaluated. Eight were YG8Pook/J animals (Friedreich ataxia phenotype) and eight wild-type mice served as controls. Auditory function was assessed between ages 6 and 12 months using otoacoustic emissions and auditory steady-state responses. At study end, motor deficit was assessed using Rotorod testing and inner ear tissue was examined. Thirty-seven individuals with Friedreich ataxia underwent auditory steady-state evoked potential assessment and response amplitudes were compared with functional hearing ability (speech perception-in-noise) and disease status was measured by the Friedreich Ataxia Rating Scale. **Results:** The YG8Pook/J mice showed anatomic and functional abnormality. While otoacoustic emission responses from the cochlear hair cells were mildly affected, auditory steady-state responses showed exaggerated amplitude reductions as the animals aged with Friedreich ataxia mice showing a 50–60% decrease compared to controls who showed only a 20–25% reduction ($F_{(2,94)} = 17.90$, $p < 0.00$). Furthermore, the YG8Pook/J mice had fewer surviving spiral ganglion neurons, indicating greater degeneration of the auditory nerve. Neuronal density was 20–25% lower depending on cochlear region ($F_{(1, 30)} = 45.02$, $p < 0.001$). In human participants, auditory steady-state response amplitudes were correlated with both Consonant–Nucleus–Consonant word scores and Friedreich Ataxia Rating Scale score. **Interpretation:** This study found degenerative changes in auditory structure and function in YG8Pook/J mice, indicating that auditory measures in these animals may provide a model for testing Friedreich ataxia treatments. In addition, auditory steady-state response findings in a clinical population suggested that these scalp-recorded potentials may serve as an objective biomarker for disease progress in affected individuals.

INTRODUCTION

Friedreich ataxia (FRDA) is the most common hereditary ataxia affecting approximately one in 29,000 Caucasians.^{1,2} The disease is the result of biallelic pathogenic variants in the *FXN* gene.³ In 96% of mutant alleles, there is an expansion of GAA trinucleotide repeats in intron 1 which causes

partial silencing of *FXN* and consequent deficits in “frataxin”—the encoded protein.² The other 4% of allele abnormalities are the result of different pathogenic variant categories. Clinical features include progressive limb/trunk ataxia, cardiomyopathy, scoliosis, and diabetes mellitus.

Hearing difficulty is another consistently reported symptom of FRDA. While sound detection is typically normal or

near-normal,^{4,5} the majority of affected individuals show progressively disordered firing in the auditory nerve and central auditory pathways (i.e., auditory neuropathy).^{4,6,7} This leads to distortion of auditory temporal cues, impaired localization ability, and abnormal perception of complex acoustic signals such as speech.^{4,8,9} Listening in background noise is particularly disrupted with most affected adults unable to hear/communicate in group situations such as classrooms or social gatherings.^{8,9} Functional hearing worsens over time and both cross-sectional and within-subject studies have suggested that changes in hearing ability mirror overall disease progression.^{4,8,10}

Function of the auditory periphery (middle ear and cochlea) is generally unaffected, but neural activity is abnormal in FRDA.⁴ Electrophysiologic assessment typically reveals absent or distorted potentials from the cochlear nerve and auditory brainstem consistent with auditory nerve axonopathy.^{4,7} This result pattern is in accordance with histological evidence showing preserved cochlear structures (organ of Corti and hair cells), but severe degeneration of both auditory and vestibular neurons within the inner ear.^{11–13}

There are several mouse models of Friedreich ataxia (including the YG8Pook/J Pook mouse) which have demonstrated a wide range of FRDA phenotypes. These include anatomical and physiological traits such as abnormally large vacuoles in dorsal root ganglia, iron deposition in the heart, and a range of functional (motor) deficits.^{14–16} To date, there have been no investigations of the auditory pathway in these animals. An appropriate mouse model could help determine if auditory function is a reliable marker for onset and progression of the disease and provide a model for testing treatments and interventions. A central aim of this study, therefore, was to investigate whether auditory deficits are present in a mouse model of FRDA and, if so, to quantify changes over time.

Our study hypotheses were as follows: (1) that electrophysiologic brainstem potentials (Auditory steady-state responses [ASSR]) would show progressive amplitude reductions in FRDA mice over time, (2) that the number of postmortem spiral ganglion neurons (SGN) in FRDA mice would be lower than control animals, (3) that ASSR amplitudes observed in each animal would be correlated with SGN population, and (4) that ASSR amplitudes in a group of people with FRDA would be correlated with functional hearing ability and overall disease progression.

SUBJECTS, MATERIALS AND METHODS

Part A: Mouse assessment

All mouse experiments in this study were approved by the Royal Victorian Eye and Ear Hospital Animal

Research Ethics Committee (Approval #10/213AR). All studies were conducted in accordance with the United States Public Health Service's Policy on Humane Care and Use of Laboratory Animals.

Mice

A total of 16 animals were used in this experiment: Eight YG8Pook/J transgenic mice (B6.Cg-Fxntm1Mkn Tg(FXN) YG8Pook/J) (JAX, Maine, USA; Stock #008398) and eight littermate wild-type (WT) mice (C57BL/6) age and sex-matched to the transgenic strain. The Pook mice were bred from those provided by Dr Mark Pook (Brunel University, Uxbridge, UK). The offspring were homozygous for the *Fxn* knockout and either homozygous or hemizygous for the human *FXN* transgene in a 1:2 ratio. These mice had a GAA repeat of 190 + 90 as described in Al-Mahdawi *et al.*,¹⁵ and were shown to have decreased expression of frataxin mRNA and protein, deficiency of Fe-S-containing enzymes, oxidative stress, and mitochondrial iron accumulation. Furthermore, these animals are known to present with physical symptoms associated with the FRDA phenotype including dysfunction of large sensory neurons, abnormal cardiac function, and diabetes.

The mice were kept in a 12-h light/dark cycle with ad libitum access to food and water. Their well-being was monitored over the course of the experiments. Body weights were measured across the duration of the study (from 6.5 months until 12.75 months of age) to give an indication of the health of the animals and an indirect marker of energy intake/motor activity.

Rotarod testing

Rotarod testing was used to assess the animal's balance and coordination by determining their ability to remain on a rotating rod as the speed of rotation increased. The test was performed when mice were 12.75 months of age. The test used a Ugo-Basille 7650 accelerating rotarod treadmill device and four trials were performed. For each trial, rotation speed was gradually increased from 4 to 40 rpm over approximately 3–5 min with a 10 min rest between each trial. The latency for each mouse to fall from the rod was recorded.

Hearing assessment

Hearing assessments in mice were performed under general anesthesia (80 mg/kg ketamine and 5 mg/kg xylazine delivered via the peritoneum). Lubricant was placed over the eyes and the health of the tympanic membrane checked via otoscopic examination. All testing was conducted in a soundproof and electrically shielded room.

Otoacoustic emissions

Distortion product otoacoustic emissions (DPOAE) were recorded when the mice were 12 months of age. Stimuli were delivered using a Smart DPOAE system, coupled to high frequency transducers (Intelligent Hearing Systems, Miami, FL, USA) and a combination sound delivery/microphone probe (10B+, Etymotic Research, Elk Grove Village, IL, USA) with a silicone probe tip (ER10D-T03; Etymotic Research) to form a closed field delivery. Two pure tone stimuli, at frequencies F1 and F2 (with intensity represented by L1 and L2), were delivered through the probe. F1 stimuli were delivered between frequencies of 2 and 32 kHz in four steps per octave, where $F1/F2 = 1.22$, and where the stimulus intensity of $L1 = L2$. To reduce noise floor, recordings were made from 16 sweeps (repetitions) with block size of 8. Recordings were made at a stimulus intensity of 80 dB SPL. The DPOAE response generated at $2F1-F2$ was used in analyses by plotting the amplitude of the response against the $F2$ stimulus frequency.

Auditory evoked potential assessments were undertaken at seven, eight, nine, and 12 months of age. In each test session, recording of auditory brainstem responses (ABRs) and auditory steady-state responses (ASSR) was performed with stimuli presented to the left ear. The test setup involved a small stimulus probe with insert ear tip placed into the mouse external auditory meatus to deliver acoustic stimuli using a system from GSI Audera (Grason-Stadler, Eden Prairie, MN) with ER3A transducers and tube phones (Etymotics Research, Elk Grove Village, IL).

Auditory steady-state evoked potentials

Auditory steady-state responses were recorded through 23-gauge hypodermic needles which were modified by removing the plastic portion and inserting a silver chloride-coated silver wire into the lumen. These modified electrodes were inserted under the scalp so that the silver wire was in contact with the skin to produce low impedance connection. The positive recording electrode was placed at the vertex of the head, the negative electrode placed on the mastoid ipsilateral to the acoustic stimuli, and the common electrode on the mastoid contralateral to the acoustic stimuli. Impedance was tested prior to recordings and recordings only commenced if impedance measures on each electrode were between 5 and 10 k Ω .

Auditory steady-state responses (ASSRs) are continuous periodic scalp potentials that can be extracted mathematically from within the EEG via Fourier transformation.^{17,18} This mathematical function determines both the phase

angle of the periodic response (phase delay relative to the stimulus envelope) and the response amplitude at the stimulus modulation frequency. Acoustic stimuli for ASSR testing in this study were 8 kHz tones amplitude modulated with depths of 35% and 50% and presented at 95.5 dB SPL. Stimulus modulation rate varied between 170 and 200 Hz and the apparent response latency was determined from linear regression of the response phase changes as per Regan.¹⁷ ASSR amplitudes (μ V) were determined for AM tones modulated at a rate of 200 Hz to optimize response recording as per Pauli-Magnus *et al.*¹⁸

Auditory brainstem responses

For ABR testing, recordings were made from 25-gauge subcutaneous needle electrodes placed at the vertex and the nape of the neck, with a ground electrode placed on the left flank. The contralateral ear was occluded using an ear mold compound (Otoform; Dreve, Unna, Germany). The acoustic stimuli were 100 μ s duration rarefaction clicks presented over 1000 repetitions at a rate of 33 Hz. Responses were filtered between 150 and 30 kHz. The resultant ABR waveform was examined to determine the presence or absence of Wave III or Wave IV and the lowest stimulus intensity (dBpSPL) at which either peak was visible, was deemed the ABR threshold.

Termination and tissue collection

Following the final recording session, the mice were killed with an overdose of sodium pentobarbitone (1000 mg/kg; Lethobarb, Virbac Australia Pty. Ltd., Milperra Australia) administered intraperitoneally and perfused transcardially with a 10 ml syringe filled with warm normal saline followed by 4°C solution of 4% paraformaldehyde (Mallinckrodt Baker Inc., Phillipsburg, USA). Left cochleae were removed postmortem and stored in 10% neutral-buffered formalin for 24 h, then decalcified over 14–21 days in 10% EDTA in PBS, and embedded in Spur's resin.

Cochlear histology

We examined the tissue from all 16 mice in the study. Cochleae were sectioned at 2 μ m in the paramodiolar plane and mounted onto slides. Sections were collected just prior to the modiolus and through to the middle of the modiolus. Every 50th section was stained with dilute acidified thionin and these sections were used for assessment of histopathology and counts of spiral ganglion neurons. Sections were digitally scanned with a x20 objective and loaded onto Panoramic Viewer (Version 1.14) for analysis. Within this program, Rosenthal's canal was

demarcated at a magnification of $\times 100$ and the area measured by the program. All SGN soma with a visible nucleolus within the nucleus in the areas of the Rosenthal's canal were counted. The density of the SGN was calculated and averaged across all five sections. The person undertaking analysis of each slide was blinded as to the genetic status of the mouse (see Sly *et al.* for detailed protocol).¹⁹

Part B: Individuals with Friedreich ataxia

This study was approved by the Human Research and Ethics Committee of the Royal Victorian Eye and Ear Hospital, Melbourne, Australia (Project #07-747H). Written consent was obtained from all participants following explanation of the nature, purpose, and likely outcomes of the research.

Thirty-seven individuals confirmed by genetic testing as being homozygous for a GAA expansion in intron 1 of the *FXN* gene were included in the study. There were 23 male and 14 female participants aged between 9.0 and 55.0 years (25.1 ± 13.3 years) at assessment. Each individual was evaluated using the Friedreich Ataxia Rating Scale (FARS),²⁰ a measure of overall disease severity, within 6 months of their audiological examination. FARS scores varied from 33.3 to 137.0 (85.6 ± 27.0) which represents a symptom severity range from mild-to-severe levels.

Behavioral and electrophysiologic assessment of auditory function was carried out on the same day. Sound detection thresholds were at normal or near-normal levels (4 frequency average hearing levels in the better ear ≤ 20 dBHL) in all cases.

Auditory steady-state response amplitude (μV) was determined for 8 kHz tones presented at 95.5 dB SPL to the better hearing ear. The stimuli were amplitude modulated at depths of 50% and 35% (as per the mouse protocol) and a modulation rate of 100 Hz was used to elicit responses from the auditory brainstem.²¹

Functional hearing ability (open-set speech perception in background noise) was evaluated using recorded Consonant–Nucleus–Consonant (CNC) words. Stimuli were presented to the better hearing ear at 65 dB SPL (RMS). A CNC word list, consisting of 50 words, was presented with a competing noise (continuous 4-talker babble) at a signal-to-noise ratio of 0 dB to replicate everyday listening conditions. Participant responses were phonetically transcribed in real time and a “percentage phonemes correct” score was determined as per Rance *et al.*⁴

Statistical analyses

For the animal data, mixed-effects repeated measures analysis of variance (ANOVA) was performed with

subject group (FRDA/WT mouse) as the between-subject factor and test session (first/second/third), stimulus characteristics (ASSR modulation depth), and hearing level (ABR threshold) as within-subject factors. In all multivariate analyses, Tukey's post hoc tests were used to assess pairwise significant differences for categorical variables where appropriate. $p < 0.05$ were considered significant. For human data, correlation analyses (Pearson's pairwise correlations) were used to determine within-subject relationships between measures.

RESULTS

Part A: Mouse findings

Body weight

The mice showed a similar degree of weight gain across age ($F_{(5,78)} = 7.44$, $p < 0.001$) with FRDA (28.0 ± 3.5 g) and controls (26.3 ± 4.7 g) having similar body weights ($F_{(1,78)} = 0.00$, $p = 0.95$) (Fig. 1A). Males were heavier than females ($F_{(1,78)} = 244.59$, $p < 0.001$).

Rotarod testing

Balance and coordination was impaired in the FRDA mice. As shown in Figure 1B, all mice increased their ability to remain on the rotarod across four trials ($F_{(3,44)} = 14.72$, $p < 0.0001$). However, FRDA mice had significantly shorter latencies to fall from the rotarod compared to controls ($F_{(1,44)} = 22.20$, $p < 0.0001$). Mean (\pm SD) latency averaged across the four trials was 170 ± 23 sec for the FRDA mice and 247 ± 33 sec and for the WT mice. The difference between the groups may have been larger as the trials were ended at 300 sec when (in most cases) the WT mice had not fallen off.

Distortion product otoacoustic emissions

Otoacoustic emissions were recordable in each subject, but response amplitudes (signal-to-noise ratio) were lower in the FRDA mice. ANOVA showed a significant group effect ($F_{(1,253)} = 18.53$, $p < 0.001$) and a borderline group \times test frequency interaction ($F_{(16,253)} = 1.69$, $p = 0.051$) suggesting that the low to mid frequency range was most affected. Tukey's post hoc analysis revealed significant ($p < 0.05$) differences in 7/9 test frequencies below 9 kHz (Fig. 2).

Auditory brainstem response threshold

Click-evoked ABR thresholds changed over the course of study—particularly in the WT mice. Analysis of variance

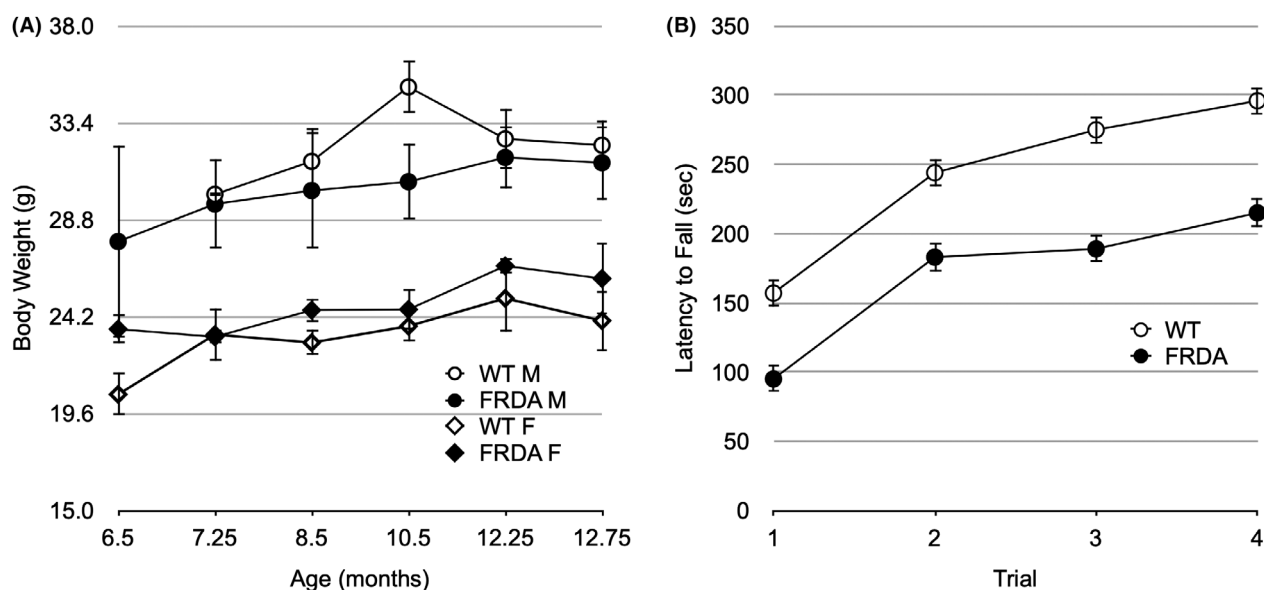


Figure 1. Mouse growth and motor function. Panel A. Body weight changes across the duration of the study. Mean \pm standard deviation body weight across each group and sex. Body weight increased across the study, with males being heavier than females. There was no difference between FRDA and control mice. Panel B. Latency to fall from rotarod at age 12.75 months. Mean \pm standard deviation fall latency across each group and sex. Fall latency increased across four trials with FRDA mice falling at significantly shorter latencies than those of control mice.

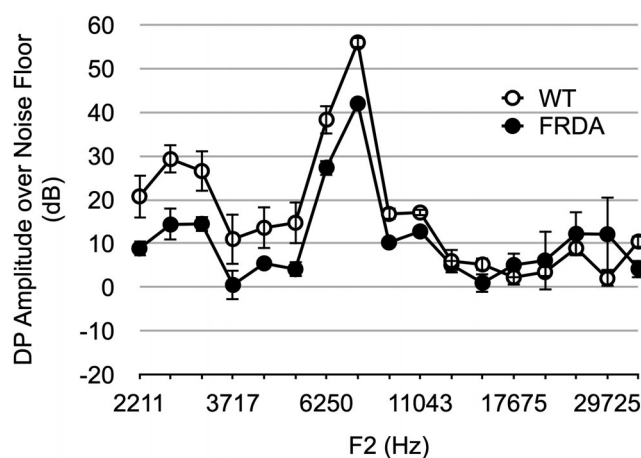


Figure 2. Distortion product otoacoustic emission amplitude (signal-to-noise ratio) as a function of test frequency for FRDA and WT mice. Responses were obtained for 80 dB SPL stimuli presented to the left ear at 12 months of age.

showed a significant deterioration across the four data collection points ($F_{(3,60)} = 3.77$, $p = 0.015$) suggesting a loss of hearing sensitivity as the mice aged. Tukey's post hoc analysis revealed no change in ABR threshold across the 7-, 8-, and 9-month data collection points ($p > 0.05$), but a significant mean difference between the 7 and 12 months data points ($p < 0.001$) (Fig. 3). As stimulus sensation level can affect auditory evoked potential amplitudes (Picton, 2010), data obtained at the 12-month collection point were excluded from subsequent analyses.

For the 7-, 8-, and 9 month sessions, there were no significant ABR threshold differences between FRDA and WT groups ($p > 0.05$).

Auditory steady-state responses

Equivalent latency

A general linear model analysis with ASSR phase difference (200–170 Hz modulation frequencies) as dependent

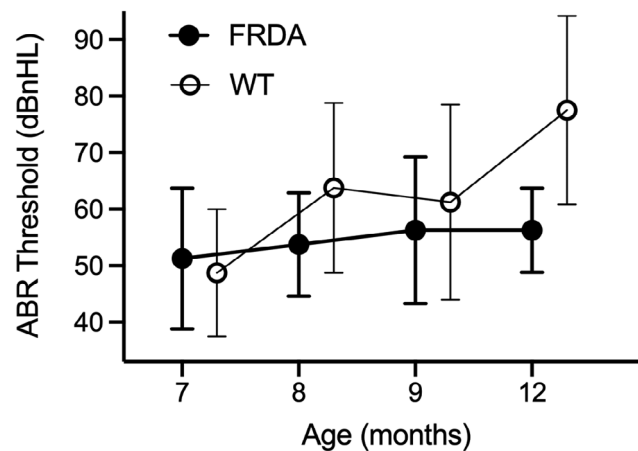


Figure 3. Click-ABR threshold levels for FRDA and WT animals across the recording period. Shown are mean \pm 2 SD values for each data collection point.

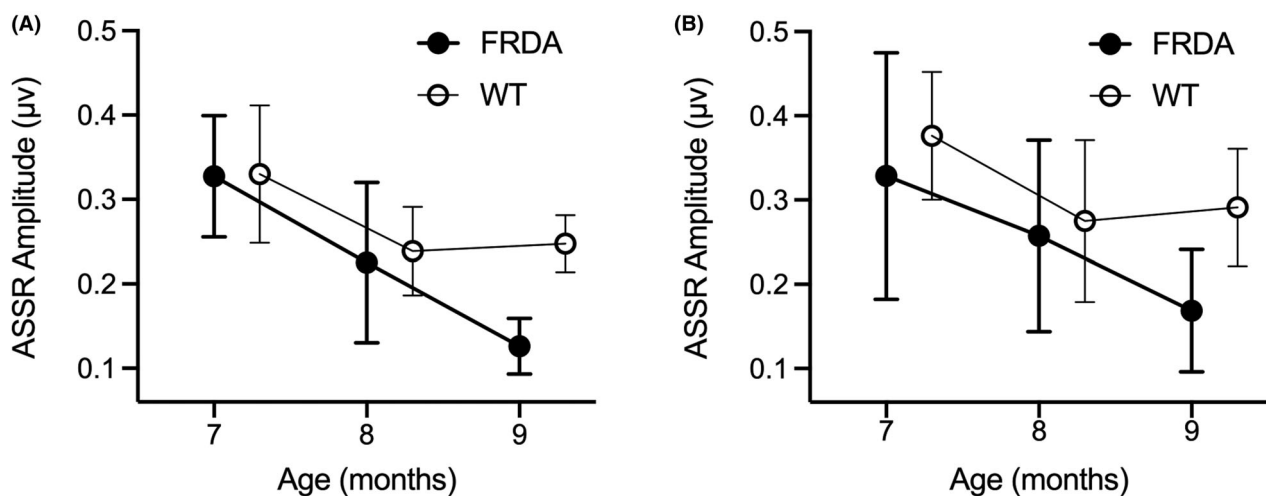


Figure 4. Auditory steady-state response amplitude levels (mean \pm 2 SD) for FRDA and WT mice across the recording period. Panel A: 35% amplitude modulation; Panel B: 50% amplitude modulation.

variable showed no effect of mouse group or test session ($p > 0.05$) so the data were combined. Mean phase difference between ASSRs elicited by 200 and 170 Hz modulation frequencies was $33.6^\circ \pm 17.0^\circ$. This corresponds to an equivalent latency of just over 3 msec:

$$\bullet \quad 33.6^\circ / 360^\circ \times 30 \text{ Hz} = 3.1 \text{ msec (Regan}^{17})$$

Auditory steady-state response amplitude

A mixed-model analysis with ASSR amplitude as dependent variable was undertaken including group, age, amplitude modulation depth, and ABR threshold as independent variables. Mouse group, AM depth, and ABR threshold were not significant in the analysis ($p > 0.05$). Subject age, in contrast, was an independent predictor

with amplitudes reducing over the course of study ($F_{(2, 94)} = 17.90$, $p < 0.001$). There were no significant interactions between factors aside from between mouse group and age at assessment with the FRDA mice showing a greater amplitude deterioration than their WT counterparts over time ($F_{(2, 94)} = 5.78$, $p = 0.005$) (Fig. 4).

Spiral ganglion neuron density

FRDA versus WT

The effect of FRDA upon the cochlear spiral ganglion neurons can be seen in Figure 5. In the FRDA mice, neuronal density was greatly reduced compared to WT counterparts ($F_{(1, 30)} = 45.02$, $p < 0.001$). Different cochlear regions (middle and apical turns) were equally affected

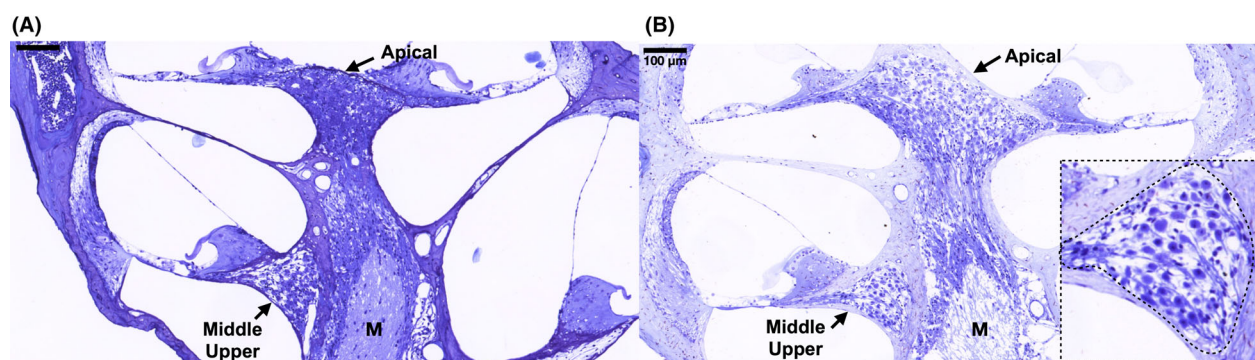


Figure 5. Spiral ganglion neuron densities in the cochlea. Panel A: typical wild-type mouse; Panel B: typical Friedreich ataxia mouse. Densities were estimated within Rosenthal's canal (curved outline in Panel B inset). Note the severe loss of spiral ganglion neurons in the Friedreich ataxia example and the reduction in auditory nerve fibers within the modiolus (M).

Table 1. Spiral ganglion neuron density (neurons/mm²) as a function of cochlear region (turn) for FRDA and WT mice.

Cochlear region	FRDA mean (SD)	WT mean (SD)	95% CI difference	p-value
Apical	1499 (329)	1994 (126)	34–956	0.039
Middle upper	1774 (277)	2262 (200)	155–820	0.010
Middle lower	1603 (230)	1993 (126)	131–649	0.009

($F_{(2, 30)} = 3.01$, $p = 0.06$). Mean SGN density values for apical, middle upper, and middle lower regions are shown in Table 1.

Relations between measures

Auditory steady-state response findings obtained for each mouse (FRDA and WT) at the final (9-month) data collection point were compared with their motor function and subsequent histologic results. Pearson's pairwise analysis showed significant correlations between ASSR amplitude (both 35% and 50% modulation depths) and Rotorod latency, with those mice showing the lowest evoked potential amplitudes also displaying the poorest balance and coordination (Table 2). Similarly, ASSR amplitudes were positively correlated with SGN counts for most cochlear regions. Rotorod latency and spiral ganglion populations were not related (Table 2).

Part B: Human data

Auditory steady-state evoked potentials

Twenty-eight of the 37 participants (75.7%) showed repeatable ASSRs to one or both amplitude modulation depths. Those with no response were allocated a response

amplitude of 0.00 μ V in subsequent analyses. Amplitudes ranged from 0.00 μ V to 0.16 μ V (0.02 ± 0.04 μ V) for the 35% stimulus modulation depth and from 0.00 μ V to 0.36 μ V (0.07 ± 0.08 μ V) for the 50% stimulus modulation depth. (Fig. 6).

Speech perception in background noise

Speech perception ability varied considerably across the clinical group and was poorer than published performance levels for neurologically normal listeners. The percentage of phonemes correctly imitated for CNC word stimuli presented (with competing noise) to each subject's better hearing ear ranged from 0.0% to 42.0% (M: $17.2 \pm 14.7\%$) (Fig. 6A). In contrast, the performance range for neurologically normal adults assessed using an identical test setup was $60.9 \pm 4.8\%$.⁴

Auditory evoked potentials, functional hearing, and FRDA severity

Auditory steady-state response findings were associated with both speech perception ability and overall disease progress. Pearson's pairwise analyses showed strong positive correlations between ASSR amplitude (both modulation depths) and phoneme score on the CNC word test (35%: $r = 0.62$, 95% CI [0.35, 0.79], $p < 0.001$; 50%: $r = 0.72$, 95% CI [0.49, 0.85], $p < 0.001$) and significant negative correlations between ASSR amplitude and FARS score (35%: $r = -0.40$, 95% CI [−0.65, −0.06], $p = 0.022$; 50%: $r = -0.53$, 95% CI [−0.74, −0.22], $p = 0.002$) (Fig. 6).

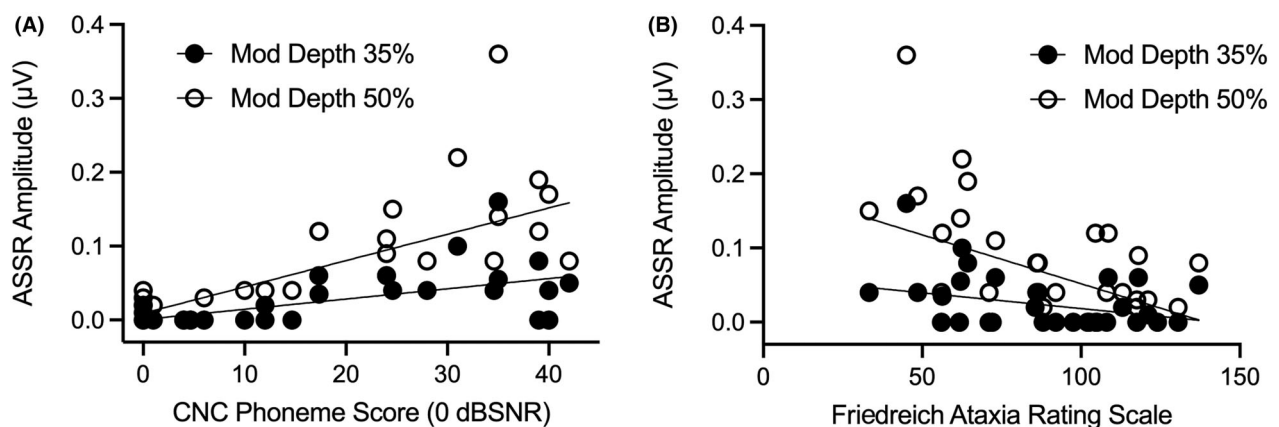
DISCUSSION

This study sought to determine whether a mouse model of FRDA would show degenerative changes in auditory

Table 2. Pearson pairwise correlations showing the association between ASSR amplitude, Rotorod latency, and SGN population in different cochlear regions.

Measure 1	Measure 2	Correlation	95% CI	p-value
Rotorod	ASSR amp (35%)	0.686	(0.245, 0.892)	0.007
Rotorod	ASSR amp (50%)	0.590	(0.087, 0.853)	0.026
SGN (apical)	ASSR amp (35%)	0.683	(0.094, 0.918)	0.029
SGN (ML)	ASSR amp (35%)	0.789	(0.360, 0.943)	0.004
SGN (MU)	ASSR amp (35%)	0.629	(0.047, 0.892)	0.038
SGN (apical)	ASSR amp (50%)	0.439	(−0.264, 0.837)	0.205
SGN (ML)	ASSR amp (50%)	0.701	(0.175, 0.916)	0.016
SGN (MU)	ASSR amp (50%)	0.855	(0.524, 0.962)	0.001
Rotorod	SGN (apical)	0.678	(−0.050, 0.936)	0.064
Rotorod	SGN (ML)	0.693	(0.054, 0.929)	0.058
Rotorod	SGN (MU)	0.431	(−0.327, 0.851)	0.247

Rotorod: Latency to fall (averaged across four trials). Apical: Apical cochlear turn. MU: Middle upper cochlear turn. ML: Middle lower cochlear turn.

**Figure 6.** Auditory steady-state response amplitude in individuals with FRDA as a function of (A) speech perception in background noise and (B) overall disability level.

structure and function as seen in people with this condition. We found abnormal auditory evoked potentials consistent with axonopathy in the cochlear nerve/brainstem and loss of spiral ganglion neurons. Furthermore, we found reduced brainstem-level potentials in individuals with FRDA where response amplitude was correlated with both auditory perception and disease severity.

Our primary outcome measure for auditory function in this study was the auditory steady-state response. This continuous, scalp potential is evoked by a periodically varying signal—typically a modulated tone. Our reasons for using the ASSR were threefold. Firstly, the potential can be extracted mathematically (by Fourier transformation) from the EEG providing an objective measure of response characteristics, without the need for subjective waveform interpretation.²² As such, the technique offers the possibility of widespread (reliable) research and clinical application. Secondly, ASSRs have been used

extensively for differential diagnosis in mouse models with a range of etiologies including cochlear hair cell loss and synaptic disorder.¹⁸ Thirdly, these responses have proven to be more robust than transient evoked potentials (such as the auditory brainstem response) in people with congenital/perinatal auditory neuropathies.²³

The ASSR can be elicited from different regions in the auditory pathway by varying the stimulus presentation frequency. For the mouse testing in this study, we employed a modulation frequency of 200 Hz which elicited a response with an equivalent latency of around 3 msec. This result is consistent with previously published mouse findings¹⁸ and suggests a cochlear nucleus origin.

Auditory steady-state responses were consistently recorded in both mouse groups, but FRDA mice showed significant amplitude reductions as the trial progressed. This deterioration is likely the result of neurodegenerative processes as preneural (cochlear) function was only mildly

affected. Otoacoustic emission responses, reflecting the cochlear mechanical processes, were recordable in each mouse at the end of the trial. Low-to-mid frequency amplitudes were slightly lower in the FRDA animals (suggesting a subtle outer hair cell abnormality in the apical cochlear turn), but overall hearing sensitivity was unaffected with equivalent ABR threshold levels obtained for FRDA and control animals throughout the recording period (Fig. 3).

Progressive reduction in auditory evoked potential amplitude is a consistent finding in humans with FRDA. While there are no published ASSR results, loss of transient brainstem potentials (ABR) has been reported in both cross-sectional studies, where response absence is more likely in patients in the latter disease stages⁸ and in studies tracking within-subject changes over time.¹⁰

There are two neurodegenerative mechanisms that might underpin ASSR amplitude deterioration. The first is *axonopathy*. Damage to auditory nerve fibers is the primary mechanism underlying auditory dysfunction in humans with FRDA.^{6,8,11} Loss of auditory axons and ganglion cells results in a deafferentation—or reduction in the amount of neural activity available to contribute to the evoked response, and hence, reduced response amplitudes.²⁴ The second potential mechanism is *dys-synchrony*. Evoked potential amplitude is also affected by the temporal precision of neural activity. This is most clearly seen with transient responses (such as the ABR) which are typically extracted from the EEG via an averaging process. This algebraic summation technique requires that the timing of neural discharges within the auditory brainstem be almost identical after each stimulus, and work by Starr *et al.* has suggested that temporal variations of as little as 0.5 msec are sufficient to make the averaged ABR unrecognizable.²⁵ Auditory steady-state responses are less dependent on temporal precision than the ABR, but ASSRs generated at the brainstem level still require that the auditory pathway be able to produce a synchronized, phase-locked response to rapid (5–6 msec) changes in the level of the stimulus. Disruption of neural firing patterns affects this representation and hence the amplitude of the ASSR may offer insights into the degree of synchrony in the distal auditory system.

Dyssynchronous neural firing may occur in FRDA as a secondary consequence of axonopathy. Loss of auditory nerve fibers produces aberrant neural firing patterns when inconsistent conduction velocities occur in damaged (but still functioning) axons.²⁶ Furthermore, because auditory nerve axons differ in their activation dynamics and adaptation properties, variations in the populations specifically affected by the axonopathy may disrupt the temporal integrity of neural firing.²⁷ In addition, secondary demyelination may occur as a consequence of axon loss and can

affect the efficiency and consistency of neural activity.²⁶ Demyelination causes slowed or irregular propagation of neural inputs and results in dys-synchrony when different fibers are affected to different degrees. Finally, demyelination can result in an impaired capacity to transmit repeated trains of pulses resulting in a partial or complete “conduction block” when decreased membrane resistance short circuits the spread of the potential along the axon.^{26,28,29}

Neural dys-synchrony in individuals with FRDA may also occur as a consequence of disease-specific differences in the myelin content of the dorsal spinal roots and distal nerves. These abnormalities are thought to result in disordered interactions between axons and Schwann cells with consequent disturbance of neural firing patterns.³⁰

Spiral ganglion neuron numbers were significantly reduced for the FRDA mice in this study. This result concurs with limited (case study) findings from individuals with FRDA. Postmortem temporal bone analyses by Spoendlin (1974) revealed a pronounced loss of SGNs in two females with FRDA. In these cases, there was no loss in the basal hook region, but counts were considerably reduced in the first cochlear turn and almost no SGNs were observed in the second and apical turns. As such, the deficits in our FRDA mice were less severe and showed a different spatial pattern (with each cochlear region similarly affected), but these animals did show clear evidence of auditory axonopathy. Furthermore, SGN counts in our study were correlated with evoked potential amplitude indicating a link between auditory structure and function in these animals.

Auditory steady-state response testing is a cornerstone of infant hearing assessment^{22,23} but has not been used to evaluate auditory function in patients with neurodegenerative disease. In order to gain insights into the possible relevance of our mouse ASSR findings, we recorded these potentials in a group of FRDA patients with a range of auditory perceptual abilities. Response amplitudes in this cohort were highly correlated with functional hearing ability (speech perception in background noise) suggesting that those individuals whose auditory pathway could more reliably encode the rapid signal amplitude changes required to generate the ASSR (i.e., those with greater a degree of auditory temporal resolution), were better able to hear and understand complex auditory signals. Furthermore, ASSR amplitudes in this group were correlated with overall disease severity suggesting that this noninvasive, scalp recorded potential may serve as an objective measure able to track the course of neurodegeneration in FRDA.

Auditory measures have shown promise as biomarkers for FRDA and other neurodegenerative diseases including Charcot–Marie–Tooth disease.²⁴ These have typically

involved speech perception assessment, taking advantage of the fact that discrimination of the subtle (<10 msec) timing cues in speech is affected by even minor changes in auditory neural firing patterns.³¹ It is for this reason that speech and communication deficits often present before (sometimes years before) motor symptoms in patients with generalized neuropathic conditions.⁷ There are, however, a number of limitations associated with the use of speech testing in populations with neurodegenerative disease. Cognitive function (which can be impaired by FRDA) may affect test scores.³² Furthermore, dysarthria, which is a common symptom of FRDA, may limit a participant's ability to produce speech sounds affecting their capacity to complete imitation-based tasks.³³ As such, an objective measure of auditory function is highly desirable. The auditory brainstem response (ABR) is not suitable as an objective biomarker for FRDA as it is unrecordable in most affected individuals from early in the disease process^{8,34} but ASSRs (which require a lesser degree of neural synchrony) may prove more useful. Further work is required, but in our clinical group, repeatable responses were obtained in >75% of participants, most of whom had previously shown absent ABRs.

Future research

The focus of this study was degenerative auditory pathway changes in mice with the FRDA genetic profile. Further work might explore anatomic and functional effects in the vestibular system. Our FRDA mice showed a loss of balance/coordination on the Rotorod test (which may be considered a form of vestibular assessment³⁵), and a correlation between Rotorod latencies and auditory function (ASSR amplitude) suggesting that the vestibular system may have been affected. Previous studies in humans have also indicated that auditory and vestibular neuropathies occur in concert in patients with a range of neurodegenerative diseases—including FRDA.^{36,37} As such, a mouse model of vestibular changes in Friedreich ataxia may provide a basis for clinical developments in humans with the disease.

In summary, this study has demonstrated the presence of auditory axonopathy and associated functional changes, in YG8Pook/J mice, suggesting that auditory measures in these animals may provide a model for evaluation of FRDA treatments. Furthermore, we have shown that ASSR assessment may provide an objective means of tracking the neurodegenerative course in patients with FRDA.

ACKNOWLEDGEMENTS

This work was supported by a Project grant from the Friedreich's Ataxia Research Alliance. GR is supported by the

Graeme Clark Chair in Audiology and Speech Science. We thank Dr Joseph Sarsero for providing the mice for this study, Mrs. Maria Clarke, Ms. Prue Nielsen, and Ms Angela Vais for histological assistance, Dr Travis Featherby for assistance with rotarod, and Mr Rodney Millard for technical assistance with electrophysiological recordings.

Conflict of Interest

The authors report no conflict of interest.

Author Contributions

Conception and design of the study—Gary Rance and David Sly; acquisition and analysis of data—Gary Rance, David Sly, Peter Carew, Leon Winata, Phillip Sale, and Martin Delatycki, and article review; drafting a significant portion of the article or figures—Gary Rance and David Sly.

Summary for Social Media

This study is the first to show degenerative auditory pathway changes in mice with the Friedreich ataxia genetic profile. The findings suggest that auditory measures may offer a model for evaluating drug treatments for the disease.

REFERENCES

1. Delatycki MB, Williamson R, Forrest SM. Friedreich ataxia: an overview. *J Med Genet.* 2000;37(1):1-8.
2. Pandolfo M. Friedreich ataxia. *Arch Neurol.* 2008;65(10):1296-1303.
3. Campuzano V, Montermini L, Molto MD, et al. Friedreich's ataxia: autosomal recessive disease caused by an intronic GAA triplet repeat expansion. *Science.* 1996;271(5254):1423-1427.
4. Rance G, Fava R, Baldock H, et al. Speech perception ability in individuals with Friedreich ataxia. *Brain.* 2008;131(8):2002-2012.
5. Koochi N, Thomas-Black G, Giunti P, Bamiou DE. Auditory phenotypic variability in Friedreich's ataxia patients. *Cerebellum.* 2021;20(4):497-508.
6. Satya-Murti S, Cacace A, Hanson P. Auditory dysfunction in Friedreich ataxia: result of spiral ganglion degeneration. *Neurology.* 1980;30(10):1047-1057.
7. Starr A, Picton TW, Sininger Y, Hood LJ, Berlin CI. Auditory neuropathy. *Brain.* 1996;119(3):741-753.
8. Rance G, Corben LA, Du Bourg E, et al. Successful treatment of auditory perceptual disorder in individuals with Friedreich ataxia. *Neuroscience.* 2010;171(2):552-555.
9. Rance G, Ryan MM, Carew P, et al. Binaural speech processing in individuals with auditory neuropathy. *Neuroscience.* 2012a;226:227-235.

10. Rance G, Corben LA, Delatycki MB. Auditory pathway changes mirror overall disease progress in individuals with Friedreich ataxia. *J Neurol*. 2012b;259(12):2746-2748.
11. Spoendlin H. Optic cochleovestibular degenerations in hereditary ataxias. II. Temporal bone pathology in two cases of Friedreich's ataxia with vestibulo-cochlear disorders. *Brain*. 1974;97:41-48.
12. Igarashi M, Miller RH, Toshiaki O, King AI. Temporal bone findings in Friedreich's ataxia. *ORL*. 1982;44(3):146-155.
13. van Bogaert L, Martin L. Optic and cochleovestibular degenerations in the hereditary ataxias. I. Clinico-pathological and genetic aspects. *Brain*. 1974;97:15-40.
14. Al-Mahdawi S, Pinto RM, Ruddle P, et al. GAA repeat instability in Friedreich ataxia YAC transgenic mice. *Genomics*. 2004;84(2):301-310.
15. Al-Mahdawi S, Pinto RM, Varshney D, et al. GAA repeat expansion mutation mouse models of Friedreich ataxia exhibit oxidative stress leading to progressive neuronal and cardiac pathology. *Genomics*. 2006;88(5):580-590.
16. Al-Mahdawi S, Pinto RM, Ismail O, et al. The Friedreich ataxia GAA repeat expansion mutation induces comparable epigenetic changes in human and transgenic mouse brain and heart tissues. *Hum Mol Genet*. 2008;17(5):735-746.
17. Regan D. Some characteristics of average steady-state and transient responses evoked by modulated light. *Electroencephalogr Clin Neurophysiol*. 1966;20(3):238-248.
18. Pauli-Magnus D, Hoch G, Strenzke N, Anderson S, Jentsch TJ, Moser T. Detection and differentiation of sensorineural hearing loss in mice using auditory steady-state responses and transient auditory brainstem responses. *Neuroscience*. 2007;149(3):673-684.
19. Sly DJ, Hampson AJ, Minter RL, et al. Brain-derived neurotrophic factor modulates auditory function in the hearing cochlea. *J Assoc Res Otolaryngol*. 2012;13(1):1-16.
20. Subramony SH, May W, Lynch D, et al. Measuring Friedreich ataxia: interrater reliability of a neurologic rating scale. *Neurology*. 2005;64(7):1261-1262.
21. Cohen LT, Rickards FW, Clark GM. A comparison of steady-state evoked potentials to modulated tones in awake and sleeping humans. *J Acoust Soc Am*. 1991;90(5):2467-2479.
22. Rance G, Rickards FW, Cohen LT, de Vidi S, Clark GM. The automated prediction of hearing thresholds in sleeping subjects using auditory steady-state evoked potentials. *Ear Hear*. 1995;16(5):499-507.
23. Rance G, Roper R, Symons L, et al. Hearing threshold estimation in infants using auditory steady-state responses. *J Am Acad Audiol*. 2005;16(5):291-300.
24. Rance G, Starr A. Pathophysiological mechanisms and functional hearing consequences of auditory neuropathy. *Brain*. 2015;138(11):3141-3158.
25. Starr A, McPherson D, Patterson J, et al. Absence of both auditory evoked potentials and auditory percepts dependent on timing cues. *Brain*. 1991;114(3):1157-1180.
26. Brown WF, Watson BV. Pathophysiology of conduction in peripheral neuropathies. In: Brown WF, Bolton CF, Aminoff MJ, eds. *Neuromuscular Function and Disease: Basic Clinical and Electrodiagnostic Aspects*. WB Saunders Company; 2002:56-95.
27. Liberman MC. Auditory-nerve response from cats raised in a low-noise chamber. *J Acoust Soc Am*. 1978;63(2):442-455.
28. Rasminsky M, Sears TA. Internodal conduction in undissected demyelinated nerve fibres. *J Physiol*. 1972;227(2):323-350.
29. Wynne DP, Zeng FG, Bhatt S, Michalewski HJ, Dimitrijevic A, Starr A. Loudness adaptation accompanying ribbon synapse and auditory nerve disorders. *Brain*. 2013;136(5):1626-1638.
30. Zouari M, Feki M, Hamida CB, et al. Electrophysiological and nerve biopsy: comparative study in Friedreich's ataxia and Friedreich's ataxia phenotype with vitamin E deficiency. *Neuromuscul Disord*. 1998;8(6):416-425.
31. Yiu EM, Tai G, Peverill RE, et al. An open-label trial in Friedreich ataxia suggests clinical benefit with high-dose resveratrol, without effect on frataxin levels. *J Neurol*. 2015;262(5):1344-1353.
32. Naeije G, Schulz JB, Corben LA. The cognitive profile of Friedreich ataxia: a systematic review and meta-analysis. *BMC Neurol*. 2022;22(1):97.
33. Brendel B, Ackermann H, Berg D, et al. Friedreich ataxia: dysarthria profile and clinical data. *Cerebellum*. 2013;12(4):475-484.
34. Rance G, Corben L, Delatycki M. Auditory processing deficits in children with Friedreich ataxia. *J Child Neurol*. 2012c;27(9):1197-1203.
35. Tung VWK, Burton TJ, Dababneh E, Quail SL, Camp AJ. Behavioral assessment of the aging mouse vestibular system. *J Vis Exp*. 2014;89:e51605.
36. Fujikawa S, Starr A. Vestibular neuropathy accompanying auditory and peripheral neuropathies. *Arch Otolaryngol Head Neck Surg*. 2000;126(12):1453-1456.
37. Maudoux A, Teissier N, Francois M, et al. Vestibular impact of Friedreich ataxia in early onset patients. *Cerebellum Ataxias*. 2020;7:6. doi:10.1186/s40673-020-00115-z